Inorganica Chimica Acta 394 (2013) 15–20

Contents lists available at SciVerse ScienceDirect

Inorganica Chimica Acta

journal homepage: www.elsevier.com/locate/ica

Synthesis, crystal structure, photoluminescence and theoretical studies of a series of copper(I) compounds based on imidazole derivatives

Tingting Hou [a,b], Jiangyu Bian [a], Xiangru Yue [b], Shumei Yue [a,*], Jianfang Ma [b]

[a] College of Chemistry, Changchun Normal University, Changchun 130032, PR China
[b] Faculty of Chemistry, Northeast Normal University, Changchun 130024, PR China

ARTICLE INFO

Article history:
Received 25 April 2012
Received in revised form 17 July 2012
Accepted 21 July 2012
Available online 31 July 2012

Keywords:
Cu(I) complexes
Crystal structure
UV–Vis spectrum
Fluorescence spectrum
DFT

ABSTRACT

Two mononuclear and one binuclear Cu(I) complexes that contain imidazole derivative ligands including 2-(2′-pyridyl)imidazole (L1), 2-(2′-pyridyl)benzimidazole(L2), and 2,6-bis (benzimidazol-2yl)-pyridine (L3) were synthesized. The formulas of these complexes are $[CuL1(PPh_3)_2][BF_4]$ (1), $[CuL2(PPh_3)_2][BF_4]$ (2), $[Cu_2(L3)_2(PPh_3)_2][BF_4]_2$ (3), respectively. The crystal structures of complexes 1–3 have been determined by single-crystal X-ray diffraction analyses. The Cu(I) ions in the complexes have a distorted tetrahedral geometry. Photophysical properties of complexes 1–3 were systematically studied. These complexes maximum emission are mainly concentrated in the 623–680 nm. An electroluminescent (EL) device using 2 as the emitter was fabricated. The device produced a red emission which matches with the PL spectrum. However, the EL device of 2 is unfavorable. The absorption properties of complexes 1 and 2 were theoretically analyzed by time-dependent density functional theory (DFT).The calculated results are in good agreement with the experimental data.

1. Introduction

Phosphorescent materials based on heavy metal complexes have great potential applications, such as light-emitting devices, solar cells, or sensors/probes [1–7]. The phosphorescence compounds of the earlier studies focused on noble Ir(III), Pt-(II), and Ru(II)complexes [8–12]. In recent years, phosphorescent Cu(I) complexes receive much attention due to relatively abundant resource and nontoxic property, which make these complexes very applicable in solar energy conversion, biological probing, and organic light-emitting devices (OLEDs) [13–18]. Zn and Cd of imidazole complexes as Blue light emitting materials have been illustrated by our research groups [19,20]. However, Cu(I) of imidazole complexes has rarely been reported. A series of Cu(I) complexes with different phosphorous/phenanthroline ligands and their electro-luminescence (EL) performances have been reported by Wang and co-workers [21]. Li and co-workers reported electroluminescent colors can be tuned ranging from green-yellow to orange-red region using Cu(I) complexes as doped material [18]. Li and co-workers reported a series of Cu(I) complexes which exhibit a maximum brightness of 4483 cd/m^2 and a peak efficiency of 3.4 cd/A [22]. Heteroleptic Cu(I) complexes comprising imidazole derivatives and triphenylphosphine (PPh_3) are promising, because they are capable of producing MLCT phosphorescent emission [23,24]. In this work, we synthesized three novel Cu(I) complexes. We obtained the crystal structure of $[CuL1(PPh_3)_2][BF_4]_2$ (1), $[CuL2(PPh_3)_2][BF_4]_2$ (2), $[Cu_2(L3)_2(PPh_3)_2][BF_4]2$ (3). We reported the preparation, crystal structure, UV–Vis spectrum, fluorescence spectrum and DFT calculation of complexes.

2. Experimental

2.1. Materials and methods

Triphenylphosphine (referred as PPh_3), pyridine-2-aldehye and pyridine-2, 6-dicarboxylic acid were purchased from Aldrich and used without further purification. The other reagents and complexes were synthesized accord to procedures. UV–Vis spectrums of samples were recorded on a TU-1901 spectrometer. Fluorescence spectra of samples were recorded on a RF-5301 spectrometer. Elemental analyses were performed on a Perkin-Elmer 240c analyzer. ^{1}H NMR spectra of samples were recorded on a Brucker AC-80 spectrometer. IR spectra of samples were recorded on a MAGNA-560 spectrometer.

2.2. Synthesis of $[CuL1(PPh_3)_2][BF_4]$

2.2.1. Synthesis of $[CuL1(PPh_3)_2][BF_4]$ (1)

In 10 mL of dichloromethane, 0.525 g (0.002 mol) PPh_3 and 0.314 g (0.001 mol) $[Cu(CH_3CN)_4]BF_4$ were dissolved and was stirred for 1 h at room temperature. After a dichloromethane solution

---

[*] Corresponding author. Tel.: +86 431 86168094.
E-mail address: yuesm458@nenu.edu.cn (S. Yue).

0020-1693/$ - see front matter © 2012 Elsevier B.V. All rights reserved.
http://dx.doi.org/10.1016/j.ica.2012.07.020

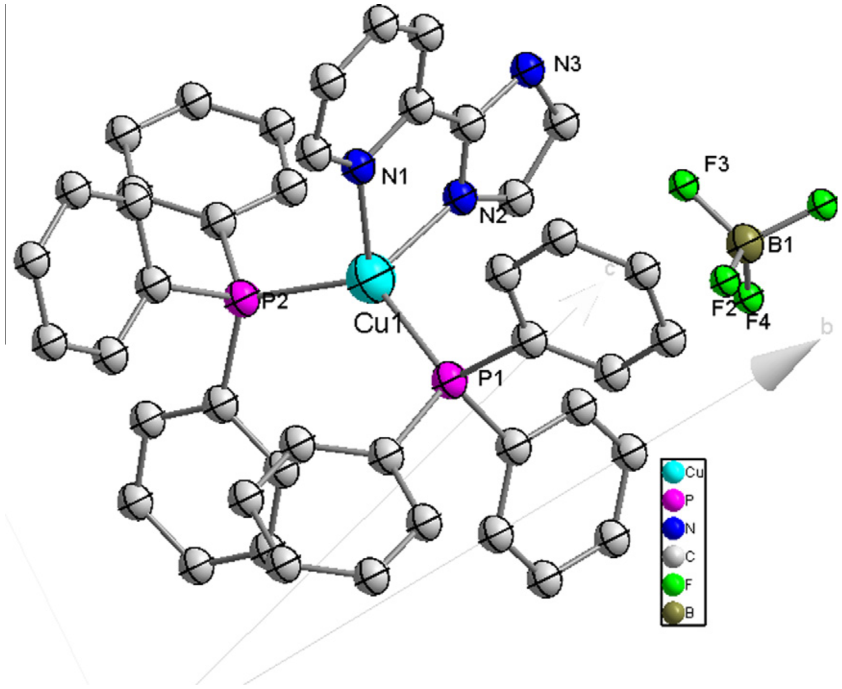

Fig. 1a. Molecule structure of complex 1.

(5 mL) of 0.135 g (0.001 mol) L1 was added, the solvent was stirred for another 4 h to give an orange solution. The solution was then filtered and evaporated to dryness. The residue was dissolved in dichloromethane and diffusion of methanol vapor into its concentrated solution gave orange crystals of 1 after 6 days (0.76 g, 78%). *Anal.* Calc. for $C_{44}H_{36}$ BCuF4N3OP2: C, 63.23; H, 4.31; N, 5.03. Found: C, 63.24; H,4.36; N, 5.05%. IR (cm^{-1}): IR (cm^{-1}): 1545, 1538, 1347, 765, 779. ^1H NMR (300 Hz, $CDCl_3$, 25 °C): δ 8.60(d, 2H, *J* = 8.0 Hz), 8.4 (d, 2H, *J* = 8.0 Hz), 8.01–7.75 (m, 20H), 7.51–7.36 (m, 12H). 31P NMR d + 1.71 (s).

2.3. Synthesis of [CuL2(PPh_3)$_2$][BF_4]

2.3.1. Synthesis of [CuL2(PPh_3)$_2$][BF_4] (2)

In 10 mL of dichloromethane, 0.525 g (0.002 mol) PPh_3 and 0.314 g (0.001 mol) [Cu(CH_3CN)$_4$]BF_4 were dissolved and was stirred for 1 h at room temperature. After a dichloromethane solution (5 mL) of 0.195 g (0.001 mol) L2 was added, the solvent was stirred for another 4 h to give an orange solution. The solution was then filtered and evaporated to dryness. The residue was dissolved in dichloromethane and diffusion of methanol vapor into its concentrated solution gave orange crystals of 2 after 7 days (0.77 g, 74%).

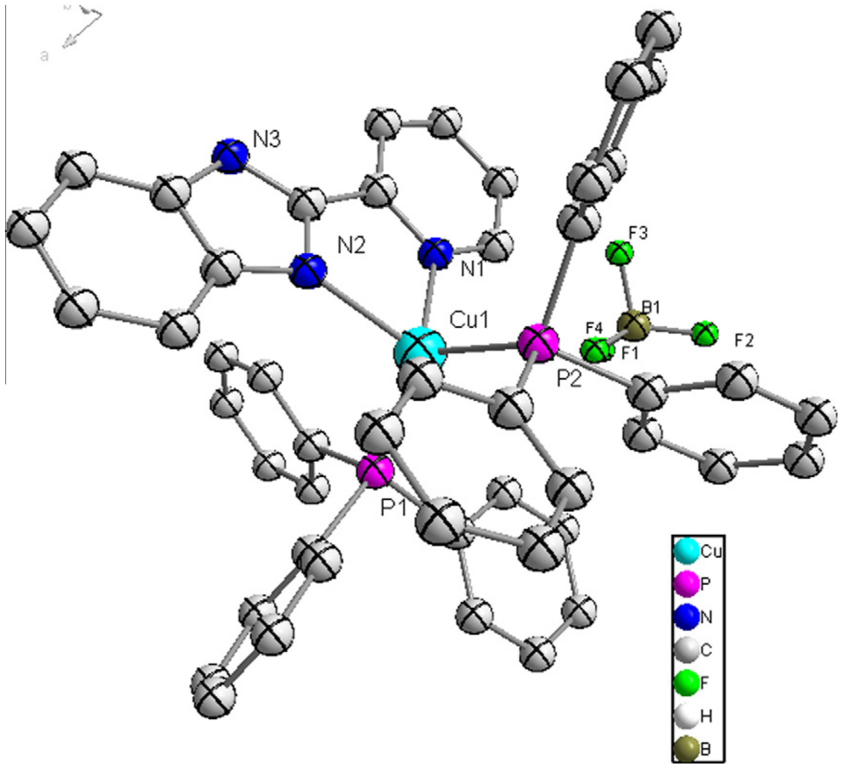

Fig. 1b. Molecule structure of complex 2.

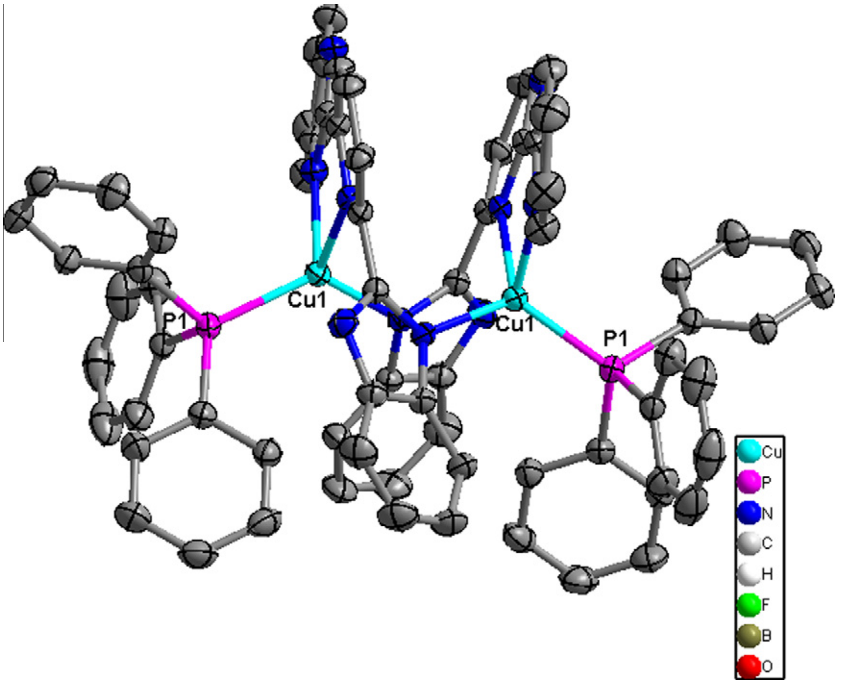

Fig. 1c. Molecule structure of complex 3.

Anal. Calc. for $C_{48}H_{37}BCuF_4N_3P_2$: C, 66.35; H, 4.26; N, 4.84. Found: C, 66.34; H,4.30; N, 4.82%. IR (cm^{-1}): 1610, 1253, 1290, 2085, 2097. ^1H NMR (300 Hz, $CDCl_3$, 25 °C): δ 8.30 (d, 2H, $J = 8.0$ Hz), 8.05 (1H, s), 7.82(1H, t), 7.26 (d, 2H,), 8.01–7.75 (m, 20H), 7.51–7.36 (m, 12H). 31P NMR d + 1.70 (s).

2.4. Synthesis of $[Cu_2(L3)_2(PPh_3)_2][BF_4]_2$

2.4.1. Synthesis of $[Cu_2(L3)_2(PPh_3)_2][BF_4]_2$ (3)

In 10 mL of dichloromethane, 0.525 g (0.002 mol) PPh_3 and 0.314 g (0.001 mol) $[Cu(CH_3CN)_4]BF_4$ were dissolved and was stirred for 1 h at room temperature. After a dichloromethane solution

Table 1
Crystal data and structure refinement for complexes 1–3.

	Complex 1	Complex 2	Complex 3
Chemical formula	$C_{44}H_{36}BCuF_4N_3OP2$	$C_{48}H_{37}BCuF_4N_3P_2$	$C_{51}H_{61}B_2Cu_2F_8N_{10}O_2P_2$
Temperature (K)	293(2)	293(2)	293(2)
Wavelength (A)	0.71069	0.71069	0.71069
Formula weight	835.05	868.10	1208.74
Space group	$P\bar{1}$	$P\bar{1}$	$C2/c$
a (Å)	10.086(5)	11.528(5)	22.2550(11)
b (Å)	14.382(5)	12.800(5)	14.9990(7)
c (Å)	15.053(5)	16.365(5)	21.6820(10)
α (°)	76.546(5)	82.421(5)	90.00
β (°)	77.955(5)	75.186(5)	99.7530(10)
γ (°)	85.186(5)	66.105(5)	90.00
V (Å^3)	2075.4(14)	2133.3(14)	7132.9(6)
Z	2	2	4
D_{calc} (mg/m^3)	1.336	1.351	1.126
Absorption coefficient (mm^{-1})	0.658	0.642	0.700
$F(000)$	858	892	2492
Crystal size (mm)	0.24 × 0.25 × 0.26	0.24 × 0.25 × 0.26	0.23 × 0.21 × 0.18
Theta range for data collection (°)	1.42 to 28.37	1.29 to 25.00	1.64 to 28.32
h	$-7 \leqslant h \leqslant 13$	$-13 \leqslant h \leqslant 7$	$-28 \leqslant h \leqslant 25$
k	$-18 \leqslant k \leqslant 18$	$-15 \leqslant k \leqslant 14$	$-15 \leqslant k \leqslant 20$
l	$-20 \leqslant l \leqslant 19$	$-19 \leqslant l \leqslant 18$	$-28 \leqslant l \leqslant 25$
Reflections collected/unique	12993/9610 [R(int) = 0.0206]	10878/7476 [R(int) = 0.0201]	22101/8680 [R(int) = 0.0275]
Completeness to θ	28.37(92.5%)	25.00(99.3 %)	25.00(99.9 %)
Absorption correction	Semi-empirical from equivalents	Semi-empirical from equivalents	Semi-empirical from equivalents
Refinement method	Full-matrix least-squares on F^2	Full-matrix least-squares on F^2	Full-matrix least-squares on F^2
Data/restraints/parameters	9610/0/235	7476/0/243	8680/12/473
Goodness-of-fit (GOF) on F^2	1.049	1.106	1.028
Final R_1, wR_2 [$I > 2\sigma(I)$]	0.0947, 0.2673	0.0960, 0.2675	0.0470, 0.1291
Final R_1, wR_2 (all data)	0.1476, 0.3164	0.1070, 0.2808	0.0742, 0.1470
$\Delta\rho_{max}$, $\Delta\rho_{min}$ (e A^{-3})	1.130, −0.846	2.442, −1.178	0.806, −0.591

(5 mL) of 0.287 g (0.001 mol) L3 was added, the solvent was stirred for another 4 h to give an orange solution. The solution was then filtered and evaporated to dryness. The residue was dissolved in dichloromethane and diffusion of methanol vapor into its concentrated solution gave orange crystals of 3 after 5 days (0.9 g, 79%). *Anal.* Calc. for $C_{51}H_{61}B_2Cu_2F_8N_{10}O_2P_2$: C, 50.63; H, 5.04; N, 11.58. Found: C, 50.62; H,5.03; N, 11.57%. IR (cm^{-1}): 1620, 1510, 1456, 762, 685. ^{1}H NMR (300 Hz, $CDCl_3$, 25 °C): δ 9.36 (d, 2H, *J* = 8.0 Hz), 8.05 (1H, s), 7.82 (1H, t), 7.26 (d, 2H,), 8.01–7.75 (m, 20H), 7.51–7.36 (m, 12H). 31P NMR d + 1.70 (s).

3. Results and discussion

3.1. Description of crystal structures

The crystal structure of complexes 1–3 are shown in Figs. 1a–1c. The Cu (I) ions in the complexes have a distorted tetrahedral geometry. Compound 1 and 2 belong to the triclinic space group $P\bar{1}$, while compound 3 belongs to the monoclinic space group *C*2/*c*. The BF_4 anions in all compounds were found to display disordering and were refined successfully. In complex 1, there is a distinct difference between the Cu–N bond lengths: the Cu(1)–N(3)(pyridyl) bond length

Table 2
Selected bond lengths (Å) and angles (°C).

		Compound 1	
Cu(1)–N(1)	2.072(5)	N(1)–Cu(1)–N(3)	80.0(2)
Cu(1)–N(3)	2.113(5)	N(1)–Cu(1)–P(1)	118.02(15)
Cu(1)–P(1)	2.2500(17)	N(3)–Cu(1)–P(1)	107.21(14)
Cu(1)–P(2)	2.2640(18)	N(1)–Cu(1)–P(2)	105.98(15)
		N(3)–Cu(1)–P(2)	109.32(14)
		P(1)–Cu(1)–P(2)	126.40(6)
		Compound 2	
Cu(1)–N(1)	2.099(5)	N(1)–Cu(1)–N(2)	80.09(18)
Cu(1)–N(2)	2.109(5)	N(1)–Cu(1)–P(2)	108.21(13)
Cu(1)–P(2)	2.2645(16)	N(2)–Cu(1)–P(2)	112.10(13)
Cu(1)–P(1)	2.2670(17)	N(1)–Cu(1)–P(1)	109.91(14)
		N(2)–Cu(1)–P(1)	109.91(13)
		P(2)–Cu(1)–P(1)	126.76(6)
		Compound 3	
Cu(1)–N(2)	2.059(2)	N(2)–Cu(1)–N(4)	96.07(9)
Cu(1)–N(4)	2.111(2)	N(2)–Cu(1)–N(3)	118.24(8)
Cu(1)–N(3)	2.167(2)	N(4)–Cu(1)–N(3)	78.32(9)
Cu(1)–P(1)	2.2084(7)	N(2)–Cu(1)–P(1)	124.12(6)
		N(4)–Cu(1)–P(1)	114.88(7)
		N(3)–Cu(1)–P(1)	113.08(6)

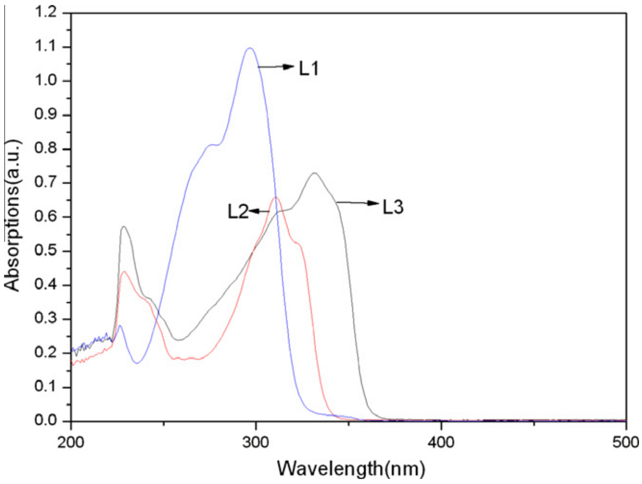

Fig. 2a. UV–Vis spectra of ligands in CH_2Cl_2 with a concentration of 1×10^{-5} mol/L.

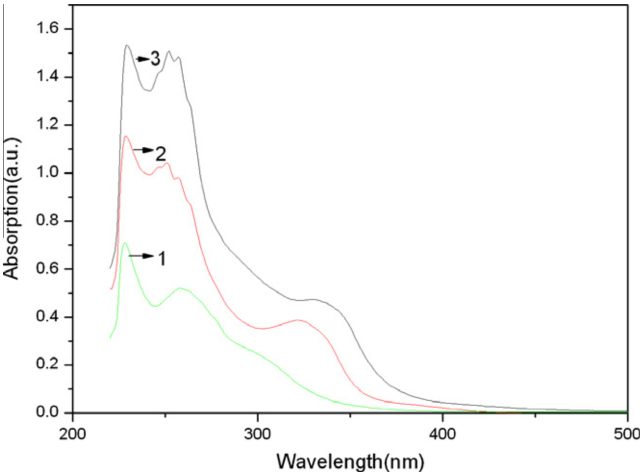

Fig. 2b. UV–Vis spectra of complexes 1–3 in CH_2Cl_2 with a concentration of 1×10^{-5} mol/L (1 is complex 1, 2 is complex 2, 3 is complex 3).

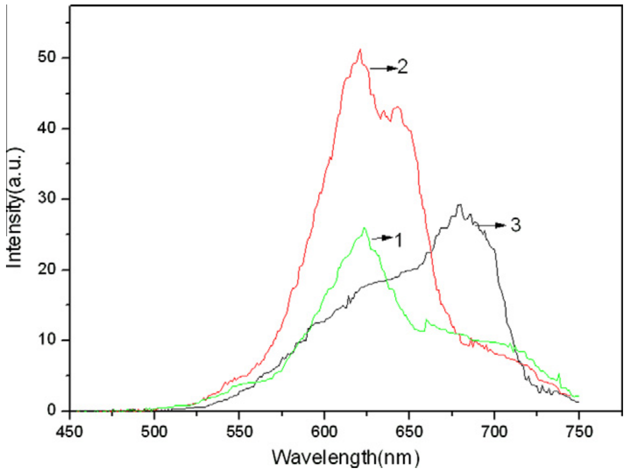

Fig. 3. Emission spectrum of complexes 1–3 in CH_2Cl_2 with a concentration of 1×10^{-5} mol/L (1 is complex 1, 2 is complex 2, 3 is complex 3).

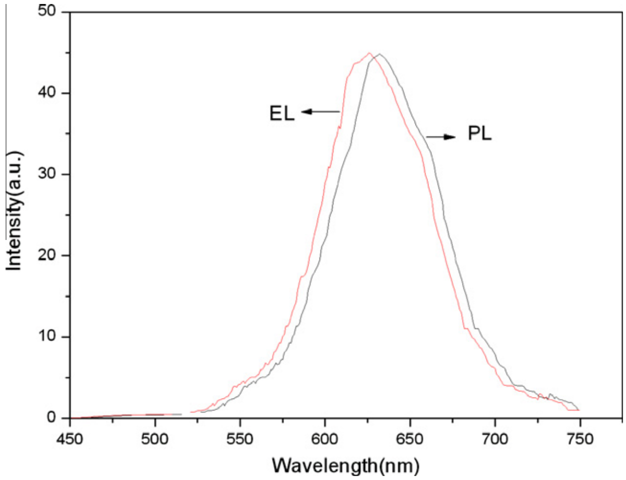

Fig. 4. The PL spectrum of 2 and EL spectra of the OLEDs based on 2 (2 is complex 2).

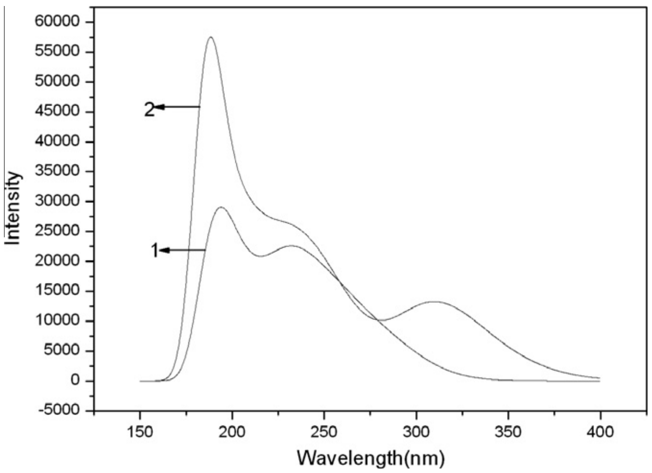

Fig. 5. Simulation absorption spectrum of complexes 1–2 (1 is complex 1, 2 is complex 2).

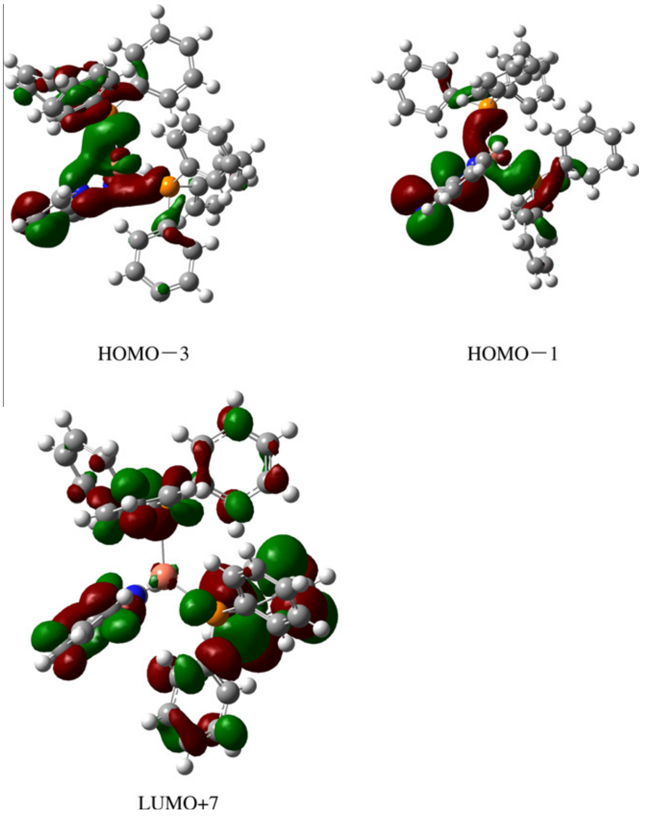

Fig. 6. Molecular orbital of complex 1.

(2.113(5) Å) is much longer than that of Cu (1)–N(1), (imidazolyl, 2.072(5) Å), indicating that the imidazolyl nitrogen atom is a stronger donor than that of the pyridyl ring. The same trend was also observed for the structures of 2 and 3 (see Table 2). Nevertheless, the observed N–Cu–N bond angles in compound 1 and 2 are similar to literature ones [17,21]. In complex 3, the central two Cu(I) ions have also an approximately tetrahedral geometry with two terminal PPh_3 ligands and two 2,6-bis(benzimidazol-2yl)-pyridine chelate. Complex 3 is a novel binuclear with N–Cu–N angles around 78.32–118.24°. The crystallographic data are given in Table 1. Selected bond lengths and angles for complexes 1–3 are listed in Table 2.

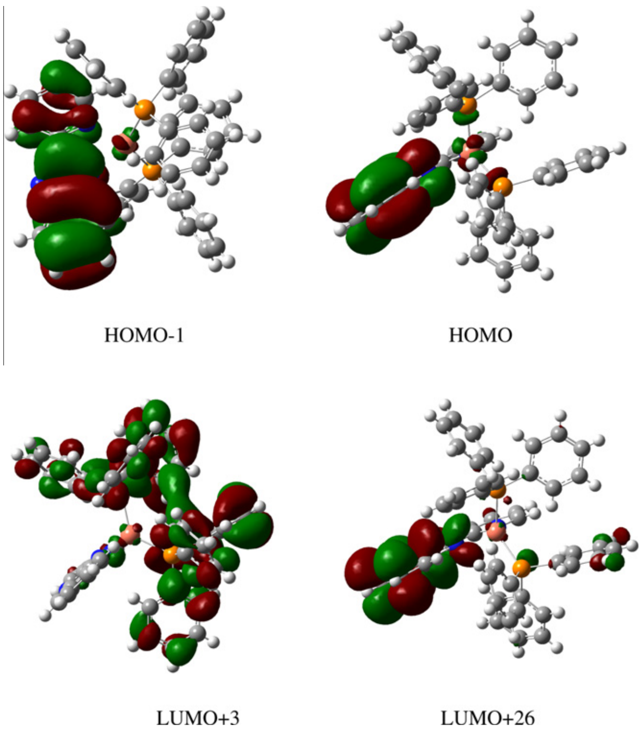

Fig. 7. Molecular orbital of complex 2.

3.2. Photophysical properties

Fig. 2a shows the UV–Vis absorption spectra of ligand L1, ligand L2, ligand L3 in dichloromethane. The free ligands L1, L2 and L3 show two absorption peaks at $\lambda_{max} \approx 230$ and 300 nm, which are probably assigned to intraligand π–π^* transitions. We found that the increase in conjugation with the nitrogen ligands, the maximum absorption has obvious red shift. Fig. 2b shows the UV–Vis absorption spectra of complexes 1–3 in dichloromethane. Compared with the ligands, complexes have a little red shift. Complexes 1–3 have multiple absorption peaks in the 220–300 nm region that can be attributed to an admixture of the intraligand π–π^* (IL) transitions of PPh_3 and the imidazole derivatives [22]. These complexes have wide and weak absorption bands in the low-energy absorption region of 300–360 nm long-wavelength range, which are tentatively assigned to the metal to ligand charge-transfer (MLCT) transitions according to the previous reports [17,23].

Fig. 3 exhibits the emission spectra of complexes 1–3 in dichloromethane. The MLCT transitions bands with the maximum value of these complexes are mainly concentrated in the 623–680 nm. The strongest emission peak of Complex 1, Complex 2 and Complex 3 are 623.0 nm, 626.0 nm and 679.0 nm, respectively [23]. We found that the increase in conjugation with the nitrogen ligands, the emission spectra has obvious red shift.

3.3. EL properties

Complex 2 was selected as a representative example for the investigation of electroluminescent properties of the Cu(I) complexes. The OLEDs utilizing complex 2 as dopants in the CBP emissive layer was fabricated with the structure of MoO_3/NPB/CBP: compound 2/TPBi.

Fig. 4 shows the PL spectrum of 2 and EL spectra for the devices based on 2 at the applied voltage of 12 V with a doping concentration of 6 wt.%. The device produced a red emission which matches with the PL spectrum. However, the EL device of 2 is unfavorable As noted by Wang and co-workers [21], the POP ligand, POP = -bis[2-(diphenylphosphino)phenyl]ether, is much better than PPh_3 ligand in Cu(I) complexes due to its increased quantum efficiency and the shortened decay lifetime. Therefore, to improve the performance of the EL devices, a modification on the ligand will be carried in our laboratory in the future.

3.4. TD-DFT

The absorption spectra of the system are computed by using TD-DFT (CAM-B3LYP) method, the Lanl2dz pseudo-potential basis sets is employed for metal atoms, and for the other atoms, the 6-311G** basis set is used. The calculated results are in good agreement with the experimental data.

The simulation absorption spectrum for the two complexes is shown in Fig. 5. Fig. 6 is molecular orbital of complex 1. The two calculated maximum absorption peak wavelength for complex 1 are 193.65 and 235.53 nm, close to the 228 and 258 nm for experimental, which correspond to the $HOMO_{-3} \rightarrow LUMO_{+7}$ and $HOMO_{-1} \rightarrow LUMO_{+7}$ transition, respectively. According to the analysis of its front molecular orbit, the $HOMO_{-3}$ is a π bonding orbit for ligand and $d_z{}^2$ for metal atom, the $HOMO_{-1}$ is a π bonding orbit for ligand and d_{yz} for metal atom, while the $LUMO_{+7}$ is a π anti-bonding orbit of ligand and $d_{x^2-y^2}$ for metal atom. So, the $\pi \rightarrow \pi^*$ transition between ligand and metal atom is the main source of the maximum absorption peak of complex 1.

For complex 2, the two calculated maximum absorption peak wavelength are 187.77 and 232.82 nm, close to the 229 and 257 nm for experimental in the high-energy absorption region. The calculated maximum absorption peak wavelength which corresponds to the HOMO → LUMO transition is 334.76 nm, close to the 326 nm for experimental in the low-energy absorption region. Fig. 7 is molecular orbital of complex 2. The absorption peak at 187.77 nm corresponds to the $HOMO \rightarrow LUMO_{+26}$ transition. As can be seen from the analysis of its front molecular orbit, the HOMO is a π bonding orbit for ligand and d_{yz} for metal atom, the $LUMO_{+26}$ is a π anti-bonding orbit of ligand and $d_{x^2-y^2}$ for metal atom. The absorption peak at 232.82 nm corresponds to the $HOMO_{-1} \rightarrow LUMO_{+3}$ transition. As can be seen from the analysis of its front molecular orbit, the $HOMO_{-1}$ is a π bonding orbit for ligand and d_{xy} for metal atom, the $LUMO_{+3}$ is a π anti-bonding orbit of ligand and d_{yz} for metal atom. So, the maximum absorption peak of complex 2, same as complex 1, is attributed to the $\pi \rightarrow \pi^*$ transition between ligand and metal atom.

4. Conclusions

In this paper, we report a series of Cu(I) complexes based on three imidazole derivatives and triphenylphosphine (PPh_3). We studied their molecular structure, electronic structure, photophysical properties and the DFT. Single crystal diffraction experiments show that the copper complex objects are distorted tetrahedral structure. The calculated results are in good agreement with the experimental data.

Acknowledgements

The authors gratefully acknowledge the financial support by the Ministry of Education of the People's Republic of China (No. 208034) and Jilin Provincial Department of Education project (Nos. 2009-203 and 2011-192).

References

[1] N. Armaroli, G. Accorsi, F. Cardinali, A. Listorti, Top. Curr. Chem. 280 (2007) 69.
[2] A.P. de Silva, D.B. Fox, T.S. Moody, S.M. Weir, Pure Appl. Chem. 73 (2001) 503.
[3] G. Accorsi, A. Listorti, K. Yoosaf, N. Armaroli, Chem. Rev. 38 (2009) 1690.
[4] P.J. Walsh, N.J. Lundin, K.C. Gordon, J.Y. Kim, C.H. Lee, Opt. Mater. 31 (2009) 1525.
[5] L. Chassot, Inorg. Chem. 23 (1984) 4249.
[6] D. Sandrini, M. Maestri, V. Balzani, L. Chassot, A. von Zelewsky, J. Am. Chem. Soc. 109 (1987) 3107.
[7] A. Vogler, H. Kunkely, Coord. Chem. Rev. 177 (1998) 81.
[8] H. Xia, C. Zhang, S. Qiu, P. Lu, J. Zhang, Y. Ma, Appl. Phys. Lett. 84 (2004) 290.
[9] X. Gong, M.R. Robinson, J.C. Ostrowski, D. Moses, G.C. Bazan, A.J. Heeger, Adv. Mater. 14 (2002) 581.
[10] X. Gong, J.C. Ostrowski, G.C. Bazan, D. Moses, A.J. Heeger, Appl. Phys. Lett. 81 (2002) 3711.
[11] S. Welter, K. Brunner, J.W. Hofstraat, L. De Cola, Nature 421 (2003) 54.
[12] Y.-L. Tung, S.-W. Lee, Y. Chi, L.-S. Chen, C.-F. Shu, F.-I. Wu, A.J. Carty, P.-T. Chou, S.-M. Peng, G.-H. Lee, Adv. Mater. 17 (2005) 1059.
[13] D.G. Cuttell, S.M. Kuang, P.E. Fanwick, D.R. McMillin, R.A. Walton, J. Am. Chem. Soc. 124 (2002) 6.
[14] S.M. Kuang, D.G. Cuttell, D.R. McMillin, P.E. Fanwick, R.A. Walton, Inorg. Chem. 41 (2002) 3313.
[15] A. Tsuboyama, K. Kuge, M. Furugori, S. Okada, M. Hoshino, K. Ueno, Inorg. Chem. 46 (2007) 1992.
[16] T. McCormick, W.L. Jia, S. Wang, Inorg. Chem. 45 (2006) 147.
[17] W.-L. Jia, T. McCormick, Y. Tao, J.-P. Lu, S.N. Wang, Inorg. Chem. 44 (2005) 5706.
[18] G. Che, Z. Su, W. Li, B. Chu, M. Li, Z. Hu, Z. Zhang, Appl. Phys. Lett. 89 (2006) 103511.
[19] S.M. Yue, N. Li, J.Y. Bian, T.T. Hou, J.F. Ma, Synth. Metals. 162 (2012) 247.
[20] S.-M. Yue, Z.-M. Su, J.-F. Ma, Y. Liao, Y.-H. Kan, H.-J. Zhang, Chin. J. Struct. Chem. 22 (2003) 174.
[21] Q. Zhang, Q. Zhou, Y. Cheng, L. Wang, D. Ma, X. Jing, F. Wang, Adv. Mater. 16 (2004) 432.
[22] Z.J. Si, J. Li, B. Li, S.Y. Liu, J. Lumin. 129 (2009) 181.
[23] L.M. Zhang, S.M. Yue, B. Li, D. Fan, Inorg. Chim. Acta 384 (2012) 225.
[24] S.-B. Zhao, T. McCormick, S.N. Wang, Inorg. Chem. 46 (2007) 10965.